Proceedings of the 25th International Conference on
Port and Ocean Engineering under Arctic Conditions
June 9-13, 2019, Delft, The Netherlands

Wave attenuation through pancake ice. Measurements from a moving vessel in the Barents Sea in 2017

Aleksey Shestov[1, 2]
[1] The University Centre in Svalbard, Longyearbyen, Norway
[2] Sustainable Arctic Marine and Coastal Technology (SAMCoT), Centre for Research-based Innovation (CRI), Norwegian University of Science and Technology, Trondheim, Norway

ABSTRACT

The knowledge about attenuation of gravitational waves in ice can be useful for offshore operations conducted in the vicinity of marginal ice zones. The length and type of ice of the marginal ice zone can vary by region and ocean conditions. There are several studies conducted in different ice condition describing attenuation of waves in ice. In this work, an absolute orientation IMU sensor was built based on open-sourced hardware and software, and it was used to obtain waves attenuation coefficients in thin, small-size pancake ice floes. The study was performed during an educational expedition of the arctic technology department at the University Centre in Svalbard. M/S Polarsyssel, the ship of the governor of Svalbard, was used 22-30 April 2017 to conduct the expedition. Wave attenuation was estimated by measuring heave response of the vessel, while it was transitioning towards ice edge across Spitsbergenbanken, the area between Hopen Island and Bjørnøya Island. A range of attenuation coefficients 0.1×10^{-4} – 0.3×10^{-4} m^{-1} was obtained for the corresponding range of wave spectra 0.1 – 0.2 Hz.

KEY WORDS: Pancake Ice, Waves, MIZ, IMU, Arduino

INTRODUCTION

The subject of waves penetration into ice cover can be of interest from different perspectives. As the sea ice cover becomes thinner and younger due to climate change (Haas et al., 2010; Kwok et al., 2009; Kwok and Rothrock, 2009; Wadhams et al., 2011) marine transportation activity and possible offshore exploitation activity in high polar regions will be increasing. At the same time, waves can penetrate deeper into ice cover and alter its state, what can be both as in favor and as against the conduction of specific marine operation. Understanding wave actions in Marginal Ice Zone and development of predictive models can contribute to run offshore operations more efficient and safe.

Field measurements of waves in the marginal ice zone (MIZ) were conducted starting in the 80s (Wadhams et al., 1988) and then several comprehensive studies were conducted on this topic in different locations and different ice conditions(Frankenstein et al., 2001; Rabault et al., 2017; Squire, 2007; Squire et al., 1995). The process of scattering of waves by ice floes depends on the type of the ice cover present and its compactness, and therefore the results

from different regions may not be fitting each other.

In 2016, Tsarau et al. (2017) performed measurements of heave responses of individual ice floes under wave conditions in the Barents sea MIZ north of Spitsbergenbanken and wave attenuation rates were obtained. Spitsbergenbanken is a sea bed area stretching from Bjørnøya northeast to Hopen and north towards the southern tip of Spitsbergen. Most of the area has depths less than 100 m. Statistical data of the last 30 years floating climatology period show that the maximum extension of ice cover goes south beyond Spitsbergenbanken (Jaklin and Berthinussen, 2015). Ice conditions in this area are of the particular interest, as this is where production license areas of petroleum activities on the Norwegian continental shelf starts (NPD, 2019). Investigations of 2016 intended to collect data of wave - ice interaction for nowadays ice conditions and to compare it with the first documented wave attenuation measurements in the same region in 1990 (Frankenstein et al., 2001). While the sizes of floes were comparable between first and recent investigations, ice thickness was considerably lower in 2016. As a result, the attenuation coefficient was found in a lower range 0.1×10^{-4} – 3.5×10^{-4} m^{-1} for the thinner ice floes than 2.0×10^{-4} – 6.0×10^{-4} m^{-1} for the thicker ice floes.

In studies of 2016 inertial measurement units (IMU) were provided by an industrial partner. Their hard affordability and some control features raised the motivation to investigate the possibility to build an IMU based on an open sourced and versatile software and hardware. The current paper describes the sensor built and a pilot attempt to measure heave responses of waves in ice and to estimate their attenuation rates. Measurements were conducted on board of M/S Polarsyssel, the vessel of the governor of Svalbard, during the annual UNIS arctic technology department expedition 22-30 April 2017 (Figure 1).

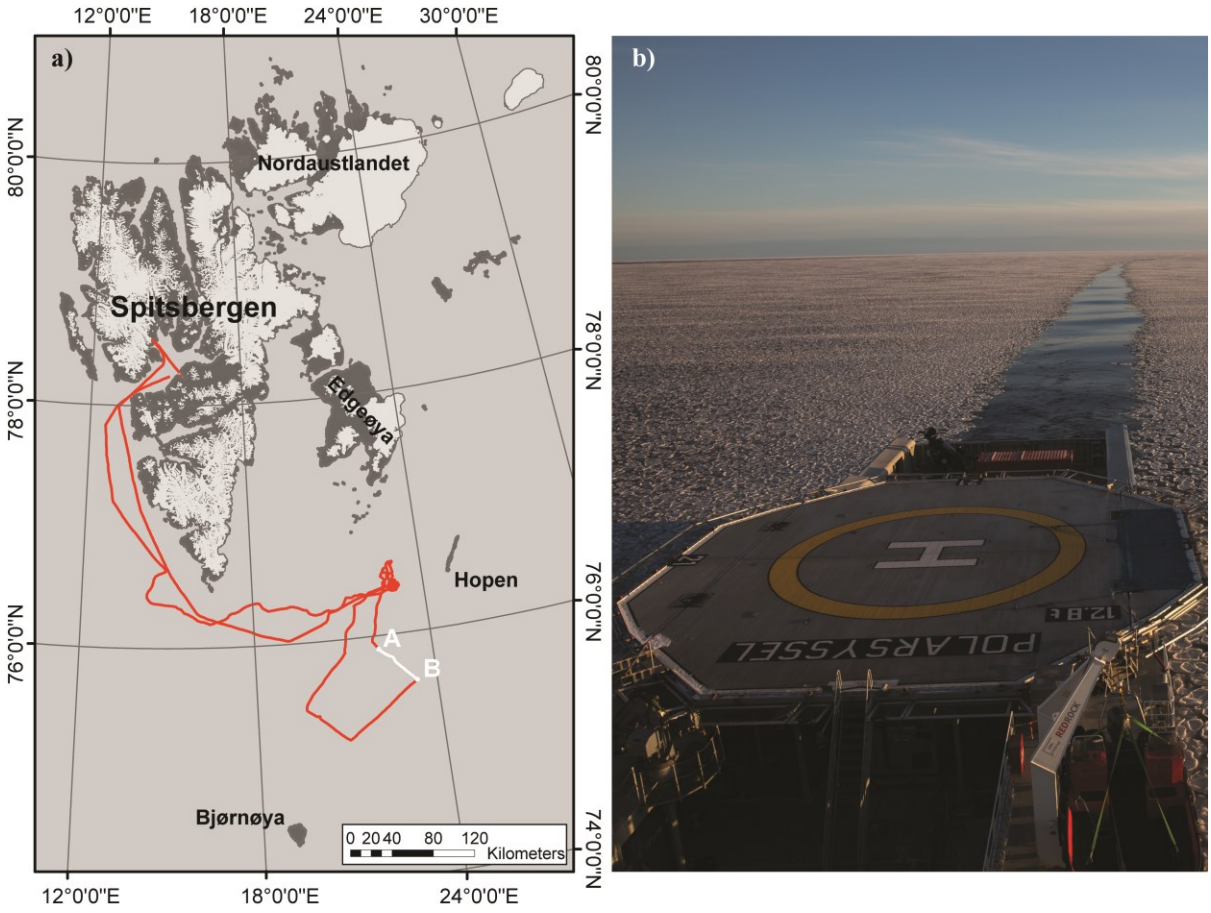

Figure 1. Track (red) of M/S Polarsyssel during UNIS expedition 22-30 April 2017. Wave measurements took place during the section of the track A-B (white) (a); M/S Polarsyssel transitioning through the pancake ice during wave measurements (b)

SENSOR

IMU was mounted using BNO055 9-axis absolute orientation sensor (BOSCH, 2019) placed by Adafruit Industries on a fusion breakout board (ADAFRUIT, 2019a) and controlled by the Arduino UNO Rev 3 open-source microcontroller (ARDUINO, 2019). Adafruit Ultimate GPS and logging shield (ADAFRUIT, 2019b) was used to enable GPS tracking and IMU sensor data being logged on microSD card. A completed set-up (Figure 2) was powered by a field power bank (external USB battery) and mounted in a watertight plastic case. Adafruit Unified BNO055 Driver for the fusion breakout board (Hoffmann, 2016), under MIT License, was used to program the sensor and was modified according to the needs. The cost of all described above, including the watertight box, is estimated at about 180 USD.

The BNO055 can output the following sensor data: angular velocity vector, magnetic field strength vector, linear acceleration vector, gravity vector and temperature at indicated sampling rates (Table 1). Though, the author encountered the conflict between GPS sensor and IMU sensor and was not able to force the controller to log data at the highest possible values.

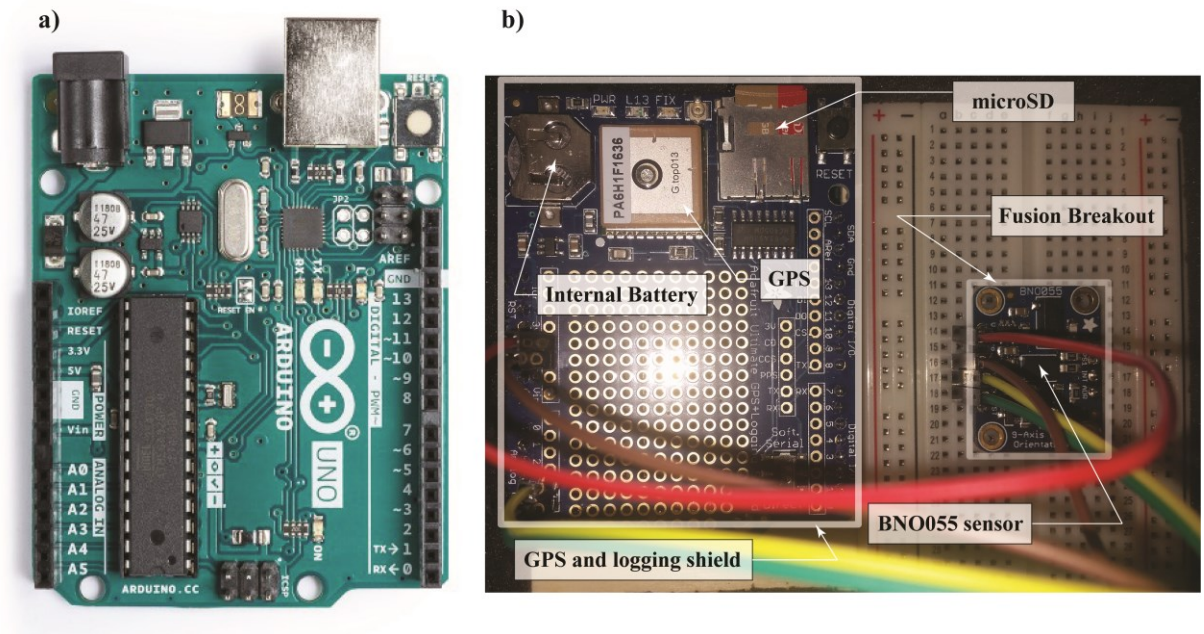

Figure 2. Arduino UNO Rev 3 microcontroller (a), Adafruit Ultimate GPS and logging shield mounted on top of Arduino UNO Rev 3 and wired Adafruit 9-DOF Absolute Orientation IMU Fusion Breakout - BNO055 (b)

Table 1. BNO055 9-axis absolute orientation sensor data output

Sensor Data	Sampling Frequency, Hz	Units	Comments
Angular Velocity Vector	100	rad/s	0
Magnetic Field Strength Vector	20	uT	0
Linear Acceleration Vector	100	m/s^2	0
Gravity Vector	100	m/s^2	0
Temperature	1	°C	0

MEASUREMENTS LOCATION AND ICE CONDITIONS

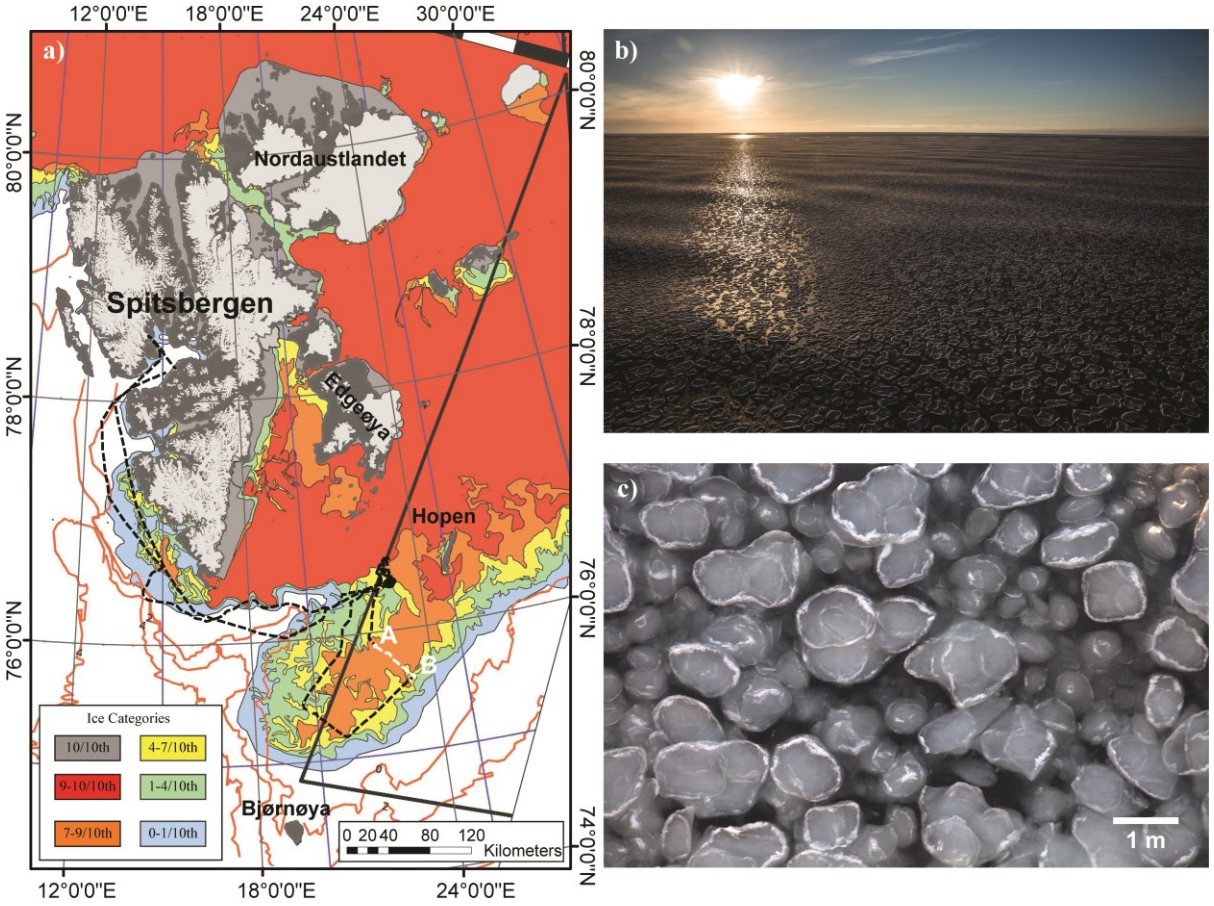

Figure 3. Ice map (NMI, 2017) around Svalbard archipelago on April 27, 2017 (a), wave conditions (b) in pancake ice cover (c).

Ice stations with studies on sea ice mechanical and physical properties were carried out east of Hopen Island at the northern edge of Spitsbergenbanken (Figure 1a). Then M/S Polarsyssel began cross sectioning of Spitsbergenbanken area to investigate potential ice formations brought out into the region from the Arctic Ocean (Figure 3). Such specific “ice tongue” just above the Spitsbergenbanken is formed by the currents system around Svalbard and Hopen Island and is common from year to year. Transitioning across this area along AB part of the track, waves propagating into ice cover from East were encountered, while ice cover was identified as a small size pancake ice (Figure 3b, c).

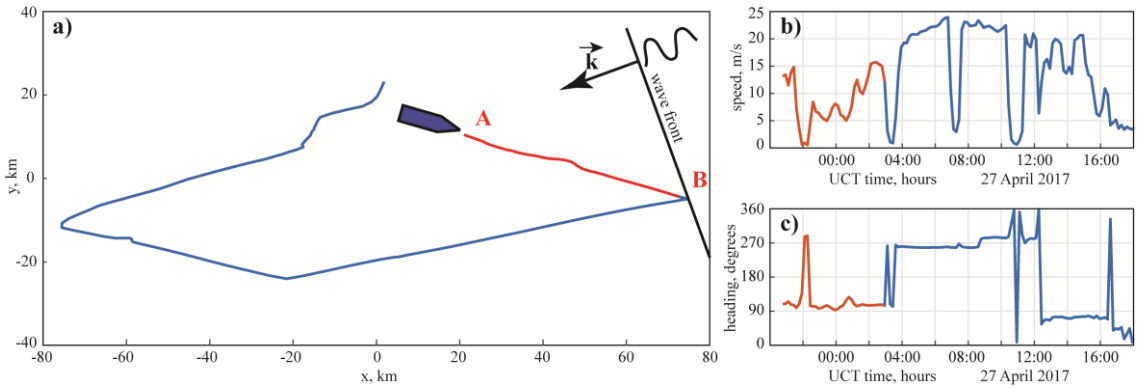

Figure 4. Track of M/S Polarsyssel in the projected system of coordinate (a), speed (b) and heading (c) of the vessel during the during transitioning across Spitsbergenbanken. Respective red segments on all graphs correspond to AB portion of the track, where wave measurements were conducted.

The vessel was moving perpendicular towards the ice edge subjected to incoming ocean waves, while incident wavefront was not parallel to ice edge (Figure 3a, Figure 4a). IMU was mounted on board of M/S Polarsyssel, and wave-induced motion of the vessel was measured along the AB segment of the track together with other vessel's motion parameters (Figure 4b, c). Difference between the vessel's heading (100°) and wave vector's heading (250°) during the AB segment resulted in wave coming from ahead at 30° on the port side of the vessel. M/S Polarsyssel was moving with speed in the range of 5-15 km/h and spent about 6 hours to pass AB segment around midnight April 27, 2019 (Figure 4b,c). In such setup, an increase of heave response was observed in time, while approaching ice edge as the vessel was heading from the ice to the open water.

DATA ANALYSIS

Linear acceleration vector and gravity vector data were used to obtain the true heave acceleration component a_z. Then the whole data series was segmented by time window of 90 seconds, and Discrete Fourier Transform was implemented to each segment of data (Figure 5). GPS position data were discretized by 10-minute intervals. Power spectral density (PSD) of heave acceleration response was averaged over 10-minute intervals accordingly. To take into account varying speed of vessel Doppler shift was implemented for each of 10 minutes intervals. Based on this, PSD of a heave acceleration response of the vessel was obtained as a function of distance along propagation of the wave. So, respective heave response of the vessel too.

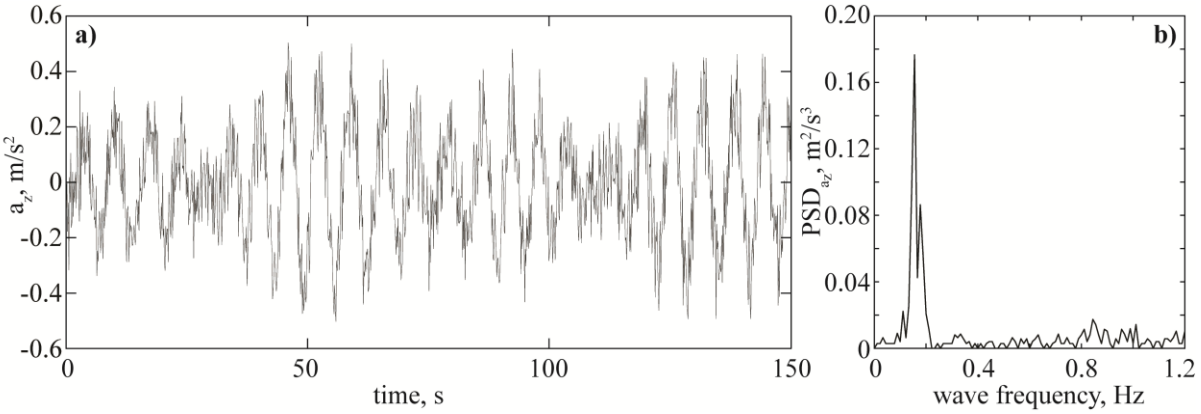

Figure 5. Example of heave acceleration component signal (a) and its power spectral density (PSD) (b)

The wave-induced heave motion of the vessel can be represented in the form of a non-dimensional response amplitude operator (RAO) defined as a ration between heave amplitude and wave amplitude. Vessel's RAO depends on the incident wavelength, incoming angle, and speed of the vessel. It is important to estimate whether the measured heave responses can be used to identify the ratios between the actual wave amplitudes at different locations, which is necessary for calculating attenuation. As to the moment, RAO's of M/S Polarsyssel are not available to the author and further analysis is only possible under the assumption that heave RAO is the same for the vessel under travel along AB segment of the track. Exact values of vessel's RAO's are not even necessary to utilize because only ratios of wave amplitudes will be further analyzed. The wave attenuation coefficient can be calculated according to Frankenstein et al. (2001):

$$\alpha = -\ln(A_2 / A_1) / (x_2 - x_1) \quad (1)$$

where α is the attenuation coefficient; A_2 and A_1 are the wave amplitudes at the two studied locations, the distance between which is ($x_2 - x_1$). In this case wave amplitude $A(x)$ exponentially decreases with distance x along the direction of wave propagation

$$A(x) = A_0 e^{-\alpha x}, \tag{2}$$

where $A_0 = A(0)$. Since energy contained in a wave over a given frequency range is proportional to the square of the wave amplitude, the ratio of the wave amplitudes A_2 / A_1 is obtained by taking the square root of the area under two corresponding PSD curves. A range of 0.011 Hz was used to generate the PSD curves for this study. Obtained from measurements, PSD data of heave acceleration response along the direction of the wave propagation were fit exponentially according to Eq.(2), and corresponding attenuation coefficients were acquired (Figure 6). For comparison, power spectral density functions of the heave acceleration component at two different distances away from the ice edge were plotted together with the wave amplitude attenuation coefficient. Note that noticeable evident attenuation of the signal in the data was observed in the cloud of data points with a range of distance to the wavefront between 17 km to 46 km. Therefore exponential fit was implemented only to those data points.

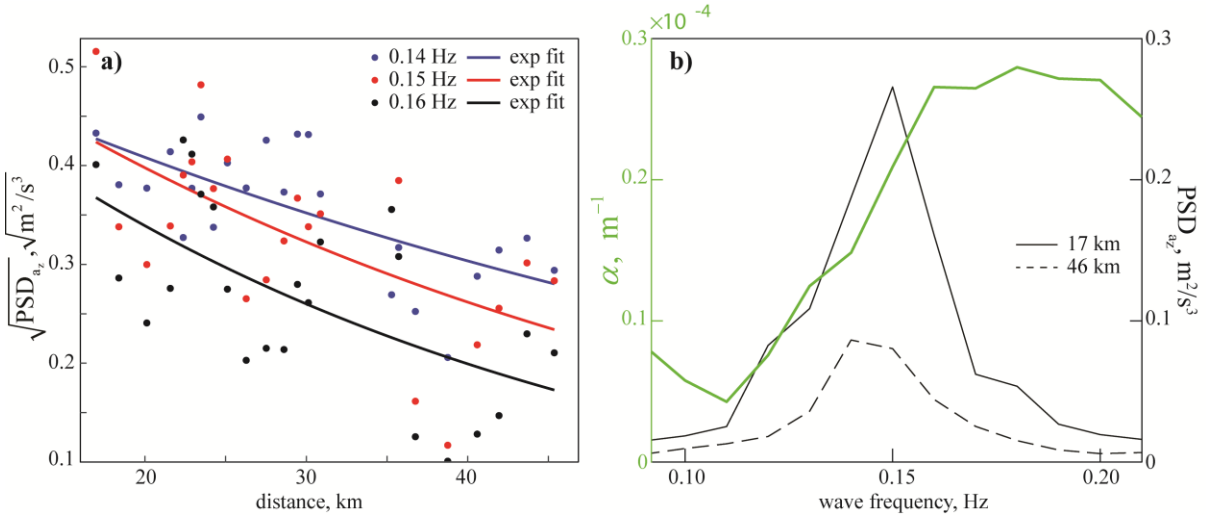

Figure 6. Exponential fit of data (square root of PSD of respective frequency range) (a) and corresponding amplitude attenuation coefficients (b). Power spectral density functions of heave acceleration at 17 and 46 km away from the ice edge (b)

DISCUSSIONS

As mentioned above, wave attenuation depends on several factors such as the type of ice present in ice cover, its overall concentration, and dimensions of single ice floes (Cheng et al., 2017). It is also indicated that the range of measured attenuation coefficients in different locations is quite broad and therefore measurements from different places may not be readily comparable with each other (Wadhams et al., 1988). Therefore a reasonable approach can be considered to compare the results with other results from similar regions and preferably comparable environmental conditions. Tsarau et al. (2017) compared their results (0.1×10^{-4} – 3.5×10^{-4} m^{-1}, ice thickness 0.2-0.4 m) obtained in 2016 with ones (2.0×10^{-4} – 6.0×10^{-4} m^{-1}, ice thickness 1.3 m) acquired by Frankenstein et al. (2001) in 1990. Considerable difference in ice thickness is in agreement with the reduction of attenuation coefficients in recent conditions.

The thickness of pancake ice described in this article was not directly measured but was estimated from images as not more than 0.1 - 0.2 m. Floes sizes varied from 0.2 m to 1.0 m; seldom pancakes were observed grouped by three or four into joint floes with size up to 2.0 m. Thus, found values ($0.1\times10^{-4} – 0.3\times10^{-4}$ m^{-1}) agree with the general trend: the thinner ice, the lower attenuation. Wadhams et al. (1988) reported a wide range ($0.2\times10^{-4} – 8.7\times10^{-4}$ m^{-1}) of attenuation coefficients for different locations and types of ice cover. The only occasion, when the range of his measurements ($0.1\times10^{-4} – 0.5\times10^{-4}$ m^{-1}) was comparable with current results, was in the Bering Sea on February 26, 1983. The ice cover then is described as open water stretches along track contained large patches of very thin ice (though, as of February 7) (Wadhams et al., 1988), which can be considered as a very similar to the conditions discussed in the current campaign. Wave frequency ranges in the Barents Sea during campaigns of Frankenstein et al. (2001), Tsarau et al. (2017) and current article were of similar values 0.1 – 0.2 Hz. During the example from the Bering Sea, when attenuation coefficients were of comparable values with the current campaign, wave frequency range was lower 0.05 – 0.1 Hz.

CONCLUSIONS

IMU was built based on sensor and controller found available at many affordable online electronic stores. Open sourced libraries were used to program the controller and run the sensor and log data. Further fixing of the program code should be done to resolve the conflict of GPS and IMU sensors to allow utilizing fully available sampling frequency. Also, modification with autonomous power supply and remote data transmitting (VHF, Satellite) can be implemented for operation in the autonomous regime. Indeed while preparing this manuscript author noted that Rabault et al. (2019) just lately released a work describing mentioned above modifications tested in the field. Starting in 2016 too, they performed a thorough development of electronic measurement equipment, and they promote the ecosystem for open source remote sensing instruments and benefit of the community at large. Thus, described in this article approach, proven to be working and to be further developed in the scientific community increasing accessibility of the sensors and reducing their costs.

Constructed IMU was tested During UNIS arctic technology department expedition 22-30 April 2017 in the Barents Sea. Attenuation of waves in pancake ice on board of M/S Polarsyssel was measured at Spitsbergenbanken between Hopen and Bjørnøya islands. A range of attenuation coefficients $0.1\times10^{-4} – 0.3\times10^{-4}$ m^{-1} was obtained for the corresponding range of wave spectra 0.1 – 0.2 Hz. Comparing with the previous measurements from the same region, attenuation coefficients are low, though the ice floes were very small too: 0.2 – 1.0 m diameter pancake ice of thickness, not more than 0.1 m.

A broad range of attenuation coefficients is reported for various ice conditions and different regions. As Cheng et al. (2017) mentions, possibly, a combined approach of field measurements in different types of ice conditions and studies in laboratories, where the number of uncertainties can be controlled, can develop a better input for the models.

ACKNOWLEDGEMENTS

This work was supported Research Council of Norway through the Centre for Research-based Innovation SAMCoT (project number 203471) and the support of all SAMCoT partners.

REFERENCES

ADAFRUIT, 2019a. Adafruit 9-DOF Absolute Orientation IMU Fusion Breakout - BNO055. Adafruit Industries (available at https://learn.adafruit.com/adafruit-bno055-absolute-orientation-sensor/overview).

ADAFRUIT, 2019b. Adafruit Ultimate GPS and Logging Shield. Adafruit Industries (available at https://learn.adafruit.com/adafruit-ultimate-gps-logger-shield/overview).

ARDUINO, 2019. Arduino UNO open-source microcontroller board. Arduino.cc (available at https://store.arduino.cc/arduino-uno-rev3).

BOSCH, 2019. BNO055 9-axis Absolute Orientation Sensor. Bosch Sensortec (available at https://www.bosch-sensortec.com/bst/products/all_products/bno055).

Cheng, S., Tsarau, A., Li, H., Herman, A., Evers, K.-U. and Shen, H., 2017. Loads on Structure and Waves in Ice (LS-WICE) Project, Part 1: Wave Attenuation and Dispersion in Broken Ice Fields, Proceedings of the 24th International Conference on Port and Ocean Engineering under Arctic Conditions, June 11-16, 2017, Busan, Korea.

Frankenstein, S., Loset, S. and Shen, H.H., 2001. Wave-Ice Interactions in Barents Sea Marginal Ice Zone. Journal of Cold Regions Engineering, 15(2): 91-102.

Haas, C., Hendricks, S., Eicken, H. and Herber, A., 2010. Synoptic airborne thickness surveys reveal state of Arctic sea ice cover. Geophysical Research Letters, 37(9).

Hoffmann, J., 2016. Adafruit Unified BNO055 Driver (AHRS/Orientation) Github (available at https://github.com/adafruit/Adafruit_BNO055).

Jaklin, G.S. and Berthinussen, I., 2015. Annual Report 2015, Norwegian Polar Institute.

Kwok, R., Cunningham, G.F., Wensnahan, M., Rigor, I., Zwally, H.J. and Yi, D., 2009. Thinning and volume loss of the Arctic Ocean sea ice cover: 2003–2008. Journal of Geophysical Research: Oceans, 114(C7): n/a-n/a.

Kwok, R. and Rothrock, D.A., 2009. Decline in Arctic sea ice thickness from submarine and ICESat records: 1958–2008. Geophysical Research Letters, 36(15).

NMI, 2017. Norwegian Ice Service. Norwegian Meteorological Institute (available at http://polarview.met.no/).

NPD, 2019. Norwegian Petrolium Derictorate FactMaps. Petroleum activities on the Norwegian continental shelf, http://gis.npd.no/factmaps/html_21/.

Rabault, J., Sutherland, G., Gundersen, O. and Jensen, A., 2017. Measurements of wave damping by a grease ice slick in Svalbard using off-the-shelf sensors and open-source electronics. Journal of Glaciology, 63(238): 372-381.

Rabault, J., Sutherland, G., Gundersen, O. and Jensen, A., 2019. An Open Source, Versatile, Affordable Waves in Ice Instrument for Remote Sensing in the Polar Regions. Pre-print (available at https://arxiv.org/abs/1901.02410v1).

Squire, V.A., 2007. Of ocean waves and sea-ice revisited. Cold Regions Science and Technology, 49(2): 110-133.

Squire, V.A., Dugan, J.P., Wadhams, P., Rottier, P.J. and Liu, A.K., 1995. Of Ocean Waves and Sea Ice. Annual Review of Fluid Mechanics, 27(1): 115-168.

Tsarau, A., Shestov, A. and Løset, S., 2017. Wave Attenuation in the Barents Sea Marginal Ice Zone in the Spring of 2016, The 24nd International Conference on Port and Ocean Engineering under Arctic Conditions, Busan, South Korea.

Wadhams, P., Hughes, N. and Rodrigues, J., 2011. Arctic sea ice thickness characteristics in winter 2004 and 2007 from submarine sonar transects. Journal of Geophysical Research: Oceans, 116(C8).

Wadhams, P., Squire, V.A., Goodman, D.J., Cowan, A.M. and Moore, S.C., 1988. The attenuation rates of ocean waves in the marginal ice zone. Journal of Geophysical Research: Oceans, 93(C6): 6799-6818.